Mechanism for vibrational relaxation in water investigated by femtosecond infrared spectroscopy

Mechanism for vibrational relaxation in water investigated by femtosecond infrared spectroscopy

Han-Kwang Nienhuys[a)]
FOM Institute for Atomic and Molecular Physics, Kruislaan 407, 1098 SJ, Amsterdam, The Netherlands and Schuit Catalysis Institute, Eindhoven University of Technology, P.O. Box 513, 5600 MB Eindhoven, The Netherlands

Sander Woutersen
FOM Institute for Atomic and Molecular Physics, Kruislaan 407, 1098 SJ, Amsterdam, The Netherlands

Rutger A. van Santen
Schuit Catalysis Institute, Eindhoven University of Technology, P.O. Box 513, 5600 MB Eindhoven, The Netherlands

Huib J. Bakker
FOM Institute for Atomic and Molecular Physics, Kruislaan 407, 1098 SJ, Amsterdam, The Netherlands

(Received 17 February 1999; accepted 30 April 1999)

We present a study on the relaxation of the O–H stretch vibration in a dilute HDO:D_2O solution using femtosecond mid-infrared pump-probe spectroscopy. We performed one-color experiments in which the $0\rightarrow1$ vibrational transition is probed at different frequencies, and two-color experiments in which the $1\rightarrow2$ transition is probed. In the one-color experiments, it is observed that the relaxation is faster at the blue side than at the center of the absorption band. Furthermore, it is observed that the vibrational relaxation time T_1 shows an anomalous temperature dependence and increases from 0.74 ± 0.01 ps at 298 K to 0.90 ± 0.02 ps at 363 K. These results indicate that the O–H···O hydrogen bond forms the dominant accepting mode in the vibrational relaxation of the O–H stretch vibration. © *1999 American Institute of Physics.* [S0021-9606(99)52028-X]

I. INTRODUCTION

In spite of its small molecular size, water is an extremely complicated liquid due to the very high density of hydrogen bonds. Due to the hydrogen-bond interactions, water exhibits many remarkable properties and is of great importance to (bio)chemistry. The hydrogen bonds strongly affect the intramolecular vibrational frequencies of the water molecule. As a result, the absorption spectrum of the O–H stretch vibration of HDO changes from a narrow band at approximately 3700 cm^{-1} in the gas phase to a broad band centered at 3400 cm^{-1} for liquid water at room temperature. There are several contributions to the broadening of this absorption band. The most important mechanism is the strong inhomogeneous broadening that results from the large distribution in the hydrogen-bond lengths. However, this inhomogeneous distribution is by no means static, since the rapid motions that take place in a liquid lead to a continuously changing environment for each water molecule. This results in rapid changes in the individual vibrational resonance frequencies of the molecules. This process is known as spectral diffusion. Another contribution is the homogeneous broadening caused by the energy relaxation of the excited O–H stretch vibration and the interactions with other degrees of freedom, such as other internal molecular vibrations or librations.

In conventional spectroscopy, such as infrared and Raman spectroscopy, it is not possible to distinguish the different contributions to the broadening of the absorption band. Time-resolved spectroscopy of the O–H stretch vibration, on the other hand, does provide a tool to measure these contributions separately. However, the interpretation of the results is often complicated due to the limited time resolution used in many experiments.[1–3]

It has been found that the O–H stretch frequency is mainly influenced by the O–H···O hydrogen bond between the hydrogen atom of the O–H group and the oxygen atom of a neighboring molecule. There exists a strong correlation between the length of this bond and the O–H stretch frequency.[4,5] Hence, the O–H stretch vibration forms a very useful probe to investigate the dynamics of the hydrogen bonds. By probing the spectral diffusion of the O–H stretch vibration, it has been found[6,7] that the length of the hydrogen bond changes on a subpicosecond time scale. This represents the time scale on which structural changes take place on a microscopic level in liquid water.

The inelastic interactions that cause the vibrational energy relaxation of the O–H stretch excitation can be probed by measuring the vibrational lifetime T_1. The modes to which the energy of the excited O–H vibration is transferred can be identified[8] by measuring the temperature dependence of T_1. Typically, a decrease of lifetime with temperature is found. Strongly different vibrational lifetimes have been reported for the O–H stretch vibration of HDO dissolved in D_2O. In a picosecond mid-infrared study using 11 ps pulses, a value for T_1 of 8 ± 2 ps was found,[1] whereas in a more recent study where pulses of 0.5 ps were used, a T_1 of 1.0

a)Electronic mail: h.nienhuys@amolf.nl

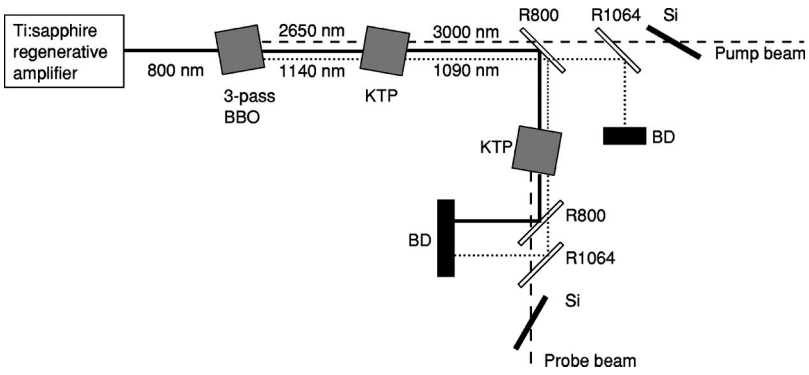

FIG. 1. Generation of 3 μm pulses. Abbreviations: BBO: BBO crystal; KTP: KTP crystal; R800: dielectric 800 nm mirror; R1064: dielectric 1064 nm mirror; Si: silicon Brewster window; BD: beam dump. See the text for further explanation.

± 0.2 ps was inferred.[9] However, in a study[2] in which the transmission was measured as a function of incident intensity, T_1 was estimated to be only 0.3–0.6 ps. In this paper, we present a detailed investigation of the relaxation mechanism of the O–H stretch vibration of HDO dissolved in D_2O using femtosecond mid-infrared pump-probe spectroscopy. In the experiments, the relaxation rate is measured as a function of temperature and both the $0\rightarrow1$ and the $1\rightarrow2$ vibrational transitions are probed. The combination of these experiments enables us to identify the vibrational relaxation mechanism.

II. EXPERIMENT

A. Infrared generation

The method of pulse generation is depicted schematically in Fig. 1. A commercial Ti:sapphire regenerative amplifier generates 800 nm, 150 fs, 1 mJ pulses at a 1 kHz repetition rate. These pulses are used to pump an optical parametric generation and amplification stage (OPG/OPA) based on a β-barium borate (BBO) crystal, that converts part of the pump energy to tunable mid-infrared pulses with typical wavelengths of 1140 nm (signal) and 2650 nm (idler). The full width at half maximum (FWHM) bandwidths of these pulses are typically 80 and 200 nm, respectively.

We use the broadband signal and the remaining 800 nm pump to seed a second OPA process in a potassium titanyl phosphate (KTP) crystal, where 800 nm light is converted to a signal wavelength at approximately 1090 nm and an idler wavelength at 3000 nm. By changing the phase-match angle of the KTP crystal, the idler wavelength can be continuously tuned up to 3300 nm with an energy of typically 20 μJ, a bandwidth of 80 nm, and a FWHM duration of 250 fs. This wavelength range corresponds to frequencies larger than 3000 cm^{-1}, which is suitable for exciting and probing the O–H stretch vibration in water. The remaining pump and signal wavelength components are removed by means of dielectric 800 and 1064 nm mirrors. Any remaining short wavelength components are filtered out by a silicon plate positioned at the Brewster angle. The infrared pulse generation is described in more detail elsewhere.[10]

To obtain a probe pulse in the one-color experiments, part of the pulse is reflected by an uncoated calcium fluoride window. In the two-color experiments, the probe pulse is generated by using part of the seed for another parametric amplification process in a second KTP crystal. In this process, an independently frequency-tunable probe pulse with an energy of 1 μJ is generated.

B. Pump-probe setup

Figure 2 shows a schematic outline of the pump-probe setup. The generated pump pulses are focused to a 200 μm-wide spot in the sample. Part of the probe pulses is split off and measured by a reference detector, in order to compensate for pulse-to-pulse fluctuations of the probe intensity. The intensities of the reference light (I_{ref}) and of the probe light transmitted by the sample (I) are measured by PbSe photoconductive cells. Using a chopper to block every other pump pulse, we calculate the probe transmission $T=I/I_{\mathrm{ref}}$ in the presence of a pump pulse and the reference transmission $T_0=I_0/I_{\mathrm{ref}}$ without a pump pulse. The absorption change, given by $\Delta\alpha=-\ln(T/T_0)$, is then measured as a function of the delay between pump and probe pulses. The probe polar-

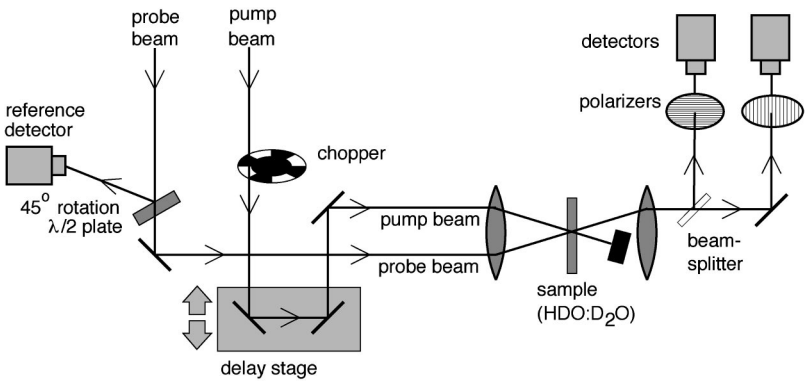

FIG. 2. Pump-probe setup. In the two-color experiments, performed at the magic angle, no polarizers were used and only one detector was placed behind the sample.

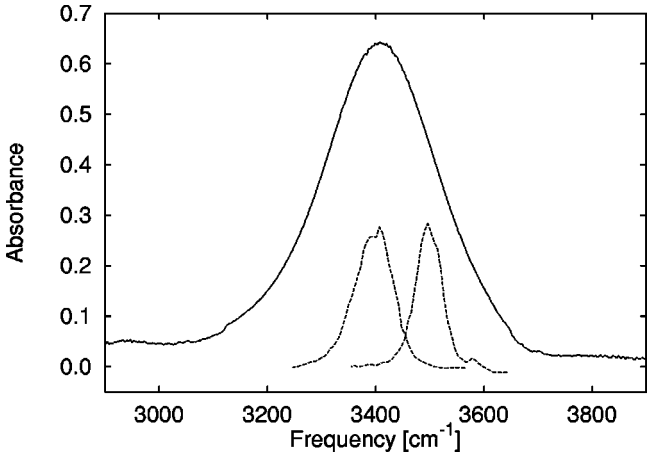

FIG. 3. Absorption spectrum of the OH-stretch band of a dilute (0.4%) HDO in D_2O solution (solid line), corrected for the D_2O background. The dashed lines indicate the excitation spectra that we used in the experiments.

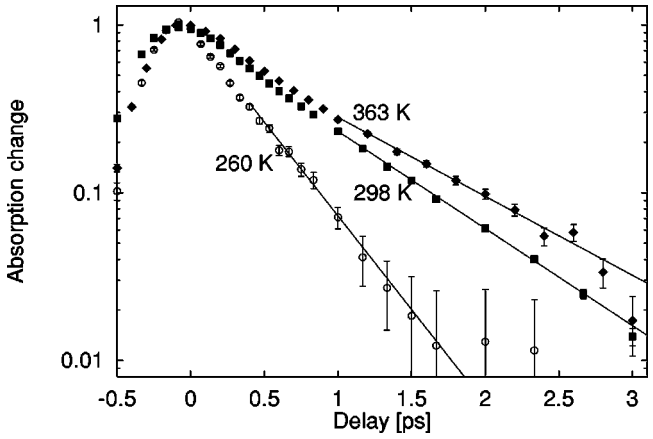

FIG. 4. Typical normalized magic angle two-color measurements on solid (260 K) and liquid (298 and 363 K) HDO in D_2O at different temperatures. In liquid water, the pump and probe frequencies were 3400 and 3150 cm^{-1}, respectively. In ice, the frequencies were 3330 and 3090 cm^{-1}, respectively.

ization is rotated by a zero-order $\lambda/2$ plate to the magic angle (54.7 deg) with respect to the pump polarization. In this way, changes in the orientation of excited molecules during the pump-probe delay will not affect the measurements.[11] This applies only if the delay between pump and probe pulses is large compared to the pulse duration. Otherwise, if the pump and probe pulses spectrally and temporally overlap, there will be a strong coherent coupling of pump and probe that leads to an additional polarization-dependent contribution to the probe signal. In the one-color measurements, the probe polarization made a 45 deg angle with the pump, and the transmissions of the perpendicular and parallel probe components were measured independently with two polarizers and two detectors. Here, the isotropic absorption change is given by $\Delta\alpha=(\Delta\alpha_{\parallel}+2\Delta\alpha_{\perp})/3$, which is equivalent to the absorption change in a magic-angle measurement. The isotropic absorption change $|\Delta\alpha|$ is typically 0.1.

The central pump frequency can be tuned within the OH-absorption band (see Fig. 3). The pump pulse excites part of the population of molecules to the excited $v=1$ vibrational state and thus induces a bleaching of the $0\rightarrow1$ transition. Due to this bleaching, a probe pulse at the same frequency as the pump that enters the sample a short time after the pump pulse will be absorbed less, whereas a probe pulse tuned to the $1\rightarrow2$ transition will have a larger absorption. The $1\rightarrow2$ absorption band is redshifted by approximately 270 cm^{-1} with respect to the $0\rightarrow1$ band, due to the anharmonicity of the OH-vibrational potential.[1]

C. Sample

The sample consisted of a 500 μm-thick layer of HDO in D_2O. The HDO concentration was chosen in such a way that the transmission at the center of the O–H absorption band was in the range 2%–8%. Thereby, a compromise was achieved between signal-to-noise ratio and maximum induced absorption change. This corresponds to a typical HDO concentration of 1%. The sample temperature was stabilized within 1 K. To prevent local heating, we rotated the sample in the one-color measurements in order to get a fresh sample for every pump pulse. The calculated temperature increase per pulse was smaller than 0.2 K. In the two-color experiments, a low pump repetition rate of 70 Hz reduced the sample heating to less than 2.5 K for a nonmoving sample.

III. RESULTS

In order to investigate the lifetime of the O–H stretch vibration, we first carried out two-color experiments in which the $0\rightarrow1$ transition is pumped and the $1\rightarrow2$ transition is probed. In Fig. 4, typical measurements at different temperatures are presented. The relaxation time can be obtained by fitting the data to a single-exponential decay. In this experiment, the time constant of the decay is equal to the vibrational relaxation time, since the absorption change is directly proportional to the excited population in the $v=1$ state.

It was found previously that for small delay times the measured signals can be influenced by effects other than the vibrational relaxation. First, the coherent coupling described in Sec. II B causes an additional signal at short delays. Second, the signals are strongly affected by spectral diffusion.[6,7] Due to the inhomogeneous broadening of the absorption band, the pump pulse will excite only a part of the absorption band, leading to the formation of a spectral hole. This spectral hole will subsequently disappear due to spectral diffusion. As a result, for pump and probe at the same frequency, the absorption change experiences an additional decrease, while for pump and probe at different frequencies there can even be an increase of the signal. It was found that in liquid water the spectral diffusion takes place on a subpicosecond time scale and is complete after 1 picosecond.[6,7] Finally, the measured signals at small delay times can be influenced by the fact that the vibrational relaxation time is likely to vary over the absorption band. However, when the spectral relaxation is complete, one will observe only one effective average decay time, independent of the probing frequency.

Because of these effects at short delay times, we fitted our data on liquid water only for delay values larger than 1.0

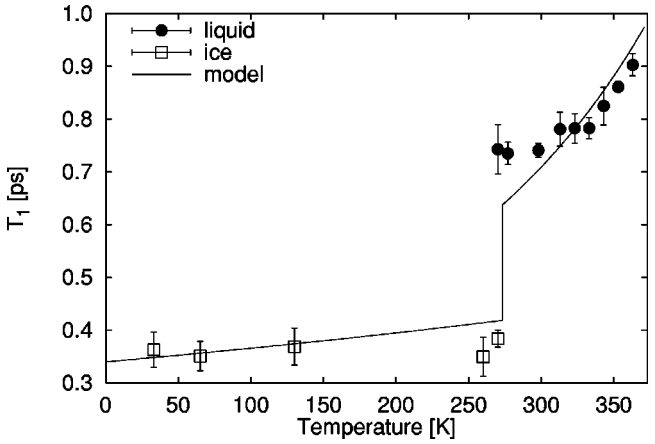

FIG. 5. Vibrational relaxation time of the OH-stretch vibration of HDO in D_2O, measured in two-color measurements. The open and closed symbols denote results in ice and liquid water, respectively. The drawn line corresponds to the model discussed in Sec. IV.

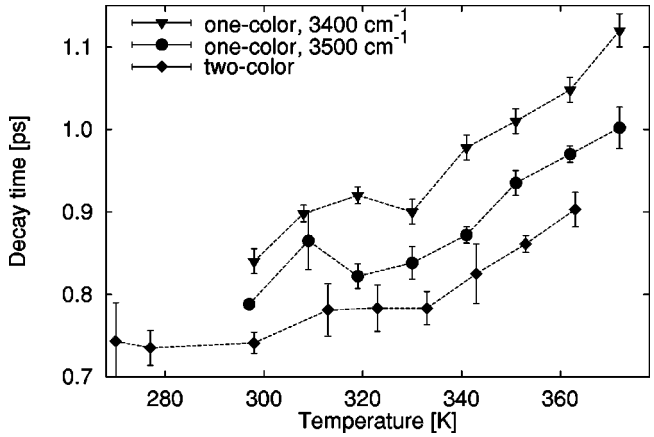

FIG. 7. Vibrational decay time constant for different temperatures as found in different experiments: one-color experiments at 3400 and 3500 cm^{-1}, and two-color experiments where the pump is at 3400 cm^{-1} and the probe at 3150 cm^{-1}.

ps. Since the relaxation in ice turns out to be much faster, we fitted the data obtained for ice only for delays larger than 0.4 ps.

Figure 5 shows the vibrational relaxation times measured in the two-color experiments for both frozen and liquid HDO:D_2O.[6] It shows that in the solid phase (ice-*Ih*), the relaxation time is virtually independent of temperature with an average value of 0.37 ± 0.02 ps, and in liquid water the relaxation time increases with temperature from 0.74 ± 0.01 ps at 270 K to 0.90 ± 0.02 ps at 363 K.

In order to obtain more information on the relaxation mechanism of the O–H stretch vibration, we also performed one-color experiments. Figure 6 shows typical measurements for one- and two-color experiments, at a temperature of 363 K. The decay times are 1.05 ± 0.02 and 0.90 ± 0.02 ps, respectively. Clearly, the one-color measurements show a slower decay.

Figure 7 shows an overview of the decay times for different frequencies and temperatures above the melting point of D_2O (277 K). It shows that for all temperatures, the decay of the absorption change $\Delta\alpha$ is slower in the one-color measurements compared to the data of the two-color experiments. Moreover, in the one-color experiments, the decay time constant is longer as the frequency is shifted from the blue side (3500 cm^{-1}) to the center (3400 cm^{-1}) of the absorption band.

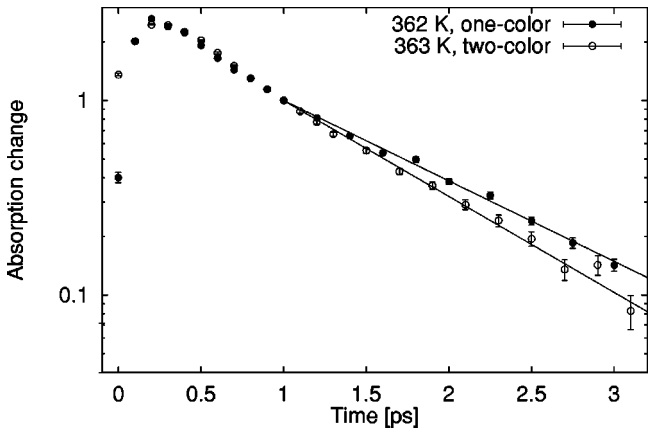

FIG. 6. Typical delay scans for the isotropic absorption change in dilute HDO:D_2O, at 363 K (two-color) and 362 K (one-color). The data are normalized at $t=1.0$ ps. The drawn lines are fits to exponentials. Note the difference in decay rates.

IV. DISCUSSION

The results from the one-color experiments at 3400 and 3500 cm^{-1}, shown in Fig. 7, suggest a frequency dependence of the vibrational relaxation time. However, due to the fast spectral relaxation, discussed in Sec. III,[6,7] this cannot cause a different decay rate of the observed signal for delays larger than 1 ps.

The slower decay found in the one-color experiments, as compared to the two-color experiments, can be explained if the excited HDO molecule does not relax directly to the ground state, but rather to an intermediate state. This can be shown as follows. The absorption for a transition $a\rightarrow b$ is given by

$$\alpha_{a\rightarrow b}=\rho\sigma_{a\rightarrow b}(n_a-n_b), \tag{1}$$

where ρ is the number of molecules per unit area, $\sigma_{a\rightarrow b}$ is the cross section for a radiative transition, and n_a and n_b are the populations of the two levels. In a two-color experiment, the decay of the pump-induced absorption change $\Delta\alpha_{1\rightarrow 2}$ only depends on the decay of n_1, since the $v=2$ state is not populated

$$\Delta\alpha_{12}(t)=\rho\sigma_{12}n_1(t). \tag{2}$$

In a one-color experiment, however, the absorption change $\Delta\alpha_{0\rightarrow 1}$ depends on both n_1 and n_0. If the growth of n_0 is not equal to the decay of n_1 due to an intermediate state, this will influence the observed relaxation.

In the following quantitative description, we label the intermediate state as $|0^*\rangle$. This intermediate state $|0^*\rangle$ is a combination of the ground state of the O–H stretch mode and other modes that are excited by accepting energy from the $v=1$ state of the O–H stretch vibration. Consequently, the $|0^*\rangle$ state can be excited to a $|1^*\rangle$ state, where both the

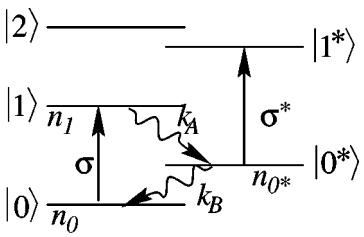

FIG. 8. States and quantities used in the analysis. The states on the left are pure excitations of the O–H vibration, while the states on the right are combinations of O–H vibrational excitations and excitations of other modes.

O–H stretch mode and the unknown other modes are excited. Due to anharmonic coupling, the center frequency of this $0^*\rightarrow 1^*$ transition can differ from the ordinary $0\rightarrow 1$ transition. Hence, the cross sections at a given laser frequency can differ. With cross sections σ^* for the $0^*\rightarrow 1^*$ and σ for the $0\rightarrow 1$ transitions, we can derive from Eq. (1) that the measured absorption change is given by

$$-\Delta\alpha_{01}(t)=\rho\sigma[2n_1(t)+(1-\sigma^*/\sigma)n_{0*}(t)]. \tag{3}$$

Clearly, the measured decay depends on the value of the cross-section ratio σ^*/σ at the probing frequency.

If the rate for the $1\rightarrow 0^*$ relaxation process is given by k_A, and for the $0^*\rightarrow 0$ relaxation by k_B (see Fig. 8), the dynamics of the population changes of the states satisfies the following equations:

$$dn_1/dt=-k_An_1, \tag{4a}$$

$$dn_{0*}/dt=k_An_1-k_Bn_{0*}, \tag{4b}$$

$$dn_0/dt=k_Bn_{0*}, \tag{4c}$$

$$n_1+n_{0*}+n_0=N, \tag{4d}$$

where N is the total number of molecules. The solutions are

$$n_1(t)=n_1(0)e^{-k_At}, \tag{5a}$$

$$n_{0*}(t)=\frac{k_A}{k_B-k_A}(e^{-k_At}-e^{-k_Bt})n_1(0)+e^{-k_Bt}n_{0*}(0), \tag{5b}$$

$$n_0(t)=N-n_1(t)-n_{0*}(t). \tag{5c}$$

We can use Eqs. (2), (3), and (5) to describe the measured decay curves. Some of the parameters are known in advance: directly after excitation, the $|0^*\rangle$ state is not populated ($n_{0*}(0)=0$). Since we are only interested in the behavior of the decay and not in the absolute value of the absorption change $\Delta\alpha$, we can set $n_1(0)=1$ and $\rho=1$. The other parameters (k_A, k_B, and σ^*/σ) must be derived from the actual data. According to Eqs. (2) and (5a), the value for k_A is directly given by the two-color experiments in which the $1\rightarrow 2$ transition is probed ($k_A=1/T_1$, as in Fig. 5). Knowing k_A, we can use the one-color data to find the values for k_B and σ^*/σ. As the difference between the one-color and two-color data is most prominent at the center of the absorption band (3400 cm^{-1}), we first attempt to fit values for k_B and σ^*/σ at that frequency. Since the two-color data were obtained at slightly different temperatures, we interpolated the k_A values linearly from the nearest temperatures above and below.

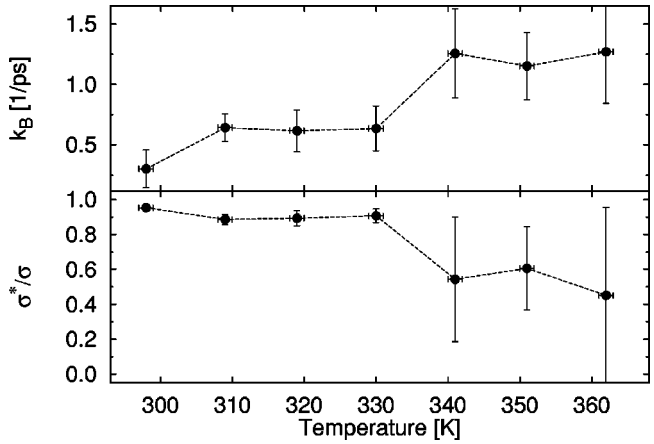

FIG. 9. The decay rate k_B and the cross-section ratio σ^*/σ as a function of temperature, resulting from a fit of the 3400 cm^{-1} data with all parameters adjustable.

The results for k_B and σ^*/σ, shown in Fig. 9, suggest that there is an increase of k_B and a decrease of σ^*/σ with temperature. However, the corresponding values for the cross-section ratio σ^*/σ at 3400 cm^{-1} are clearly anticorrelated to k_B. This probably has no physical reasons, but is due to the fact that the parameters σ^*/σ and k_B are to a certain degree exchangeable in the model: a larger value of σ^*/σ can compensate the effect of a smaller value for k_B with hardly any difference in the fit quality.

In fact, it is reasonable to assume that the cross-section ratio σ^*/σ does not depend strongly on temperature. The vibrational relaxation of the O–H vibration leads to a transfer of approximately 3400 cm^{-1} to a few accepting modes. If there were only one accepting mode, the resulting degree of excitation of this mode would correspond to a thermal distribution at a temperature of approximately 5000 K. Hence, we expect that the comparatively small range of temperatures in our measurements will not have much influence on the cross-section ratio σ^*/σ of the intermediate level, and we assume that σ^*/σ has a constant value. Since the error bars in Fig. 9 are clearly not representative for the actual uncertainty in σ^*/σ, we assume that $\sigma^*/\sigma=0.75$, which is the unweighted average of the data shown in Fig. 9. We use this value as a fixed parameter to fit all data with pump and probe frequency at 3400 cm^{-1}. This yields values for k_B as a function of temperature, as shown in the upper half of Fig. 10. With this approach, there is clearly no significant temperature dependence. Using these k_B values, we can now fit the cross sections at the 3500 cm^{-1} probe frequency, as shown in Fig. 10. At 3500 cm^{-1}, the cross section σ^* is systematically larger compared to 3400 cm^{-1}, again with no significant temperature dependence. This confirms that both k_B and σ^*/σ are independent of temperature within the error. However, the uncertainty in σ^*/σ of approximately ± 0.2 causes an error in the value of k_B. By repeating the procedure for the 3400 cm^{-1} data with $\sigma^*/\sigma=0.75-0.20$ and with $\sigma^*/\sigma=0.75+0.20$, we find that $k_B=1.0\pm 0.5$ ps^{-1}. In all

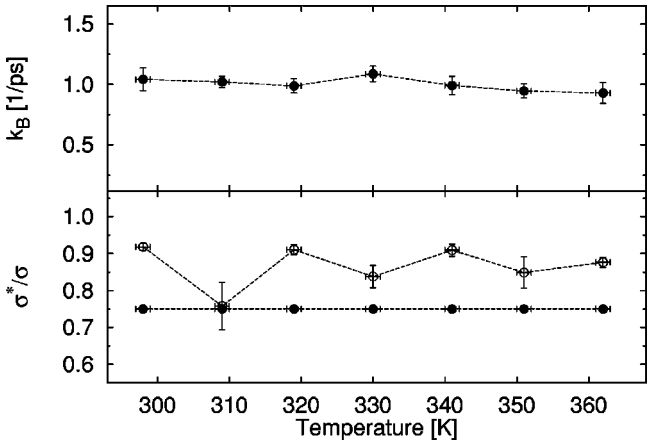

FIG. 10. The decay rate k_B and the cross-section ratio σ^*/σ as a function of temperature. In the upper half, the decay rate k_B that results from fitting the data at 3400 cm^{-1} is shown, with the cross-section ratio σ^*/σ fixed at 0.75. These k_B values are used to find the cross sections at 3500 cm^{-1} in the bottom half (open symbols). For comparison, the fixed cross section at 3400 cm^{-1} is shown as well (closed symbols).

three cases, however, we find that the cross section at 3500 cm^{-1} is systematically larger than the cross section at 3400 cm^{-1}.

The systematically larger cross sections at 3500 cm^{-1} compared to 3400 cm^{-1} suggest that the $0^* \rightarrow 1^*$ transition has a blueshifted frequency with respect to the normal O–H stretch excitation. This is quite surprising, since excitation of other anharmonically coupled molecular modes leads normally to a redshift of the vibrational frequency.[12,13] However, the blueshift can be well explained if the $|0^*\rangle$ state is an O–H stretch $v=0$ state in combination with a highly excited or even dissociated hydrogen bond. The $|1^*\rangle$ state then corresponds to the case where both the hydrogen bond and the O–H bond are excited. A qualitative picture of the energy levels involved is shown in Fig. 11. We must note here that it is a conceptual simplification to regard the $|0^*\rangle$ state as a single energy level. A more accurate description would involve a broad band of hydrogen bond energy levels, each of which causes a different blueshift and cross section of the O–H stretch transition. In principle, application of such a model would give more detailed information on the lifetime of each individual excited quantum state of the hydrogen bond. However, the fact that the data can be described satisfactorily with a single intermediate state $|0^*\rangle$ and a single relaxation rate constant $k_B = 1.0 \pm 0.5$ ps^{-1} shows that our experimental limitations do not allow us to obtain information about these more subtle details. Therefore, we limit ourselves to a lifetime for the average excitation level of the hydrogen bond.

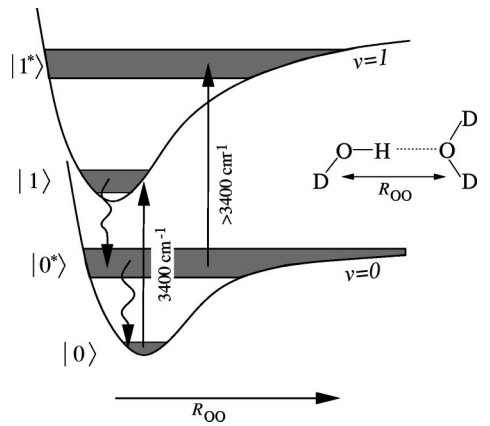

FIG. 11. Schematic potentials for the hydrogen bond, for the $v=0$ and $v=1$ O–H stretch modes. Shown are the proposed $|0\rangle$, $|1\rangle$, $|0^*\rangle$, and $|1^*\rangle$ states, the central excitation frequencies and the nonradiative decay paths.

Furthermore, there may be more relaxation channels, which possibly lead to a different frequency shift. However, other relaxation channels in which the main part of the energy is transferred to other modes, e.g., the bending mode, would lead to a transient redshift instead of a blueshift.[12,13] This suggests that other relaxation paths only contribute weakly to the relaxation of the $v=1$ state.

With the hydrogen bond as the dominant accepting mode, the anomalous temperature dependence of the vibrational relaxation time T_1 can also be explained. A theoretical model of the energy transfer from the O–H stretch vibration to the O–H···O hydrogen bond was developed by Staib and Hynes.[5] Their model system consists of a single O–H bond coupled to a single hydrogen bond. The coupling is described by Lippincot–Schroeder potentials, that incorporate the gas-phase O–H-bond potential, the hydrogen bond, and the van der Waals and electrostatic interactions. In the condensed phase, the hydrogen bond causes a redshift of the O–H stretch frequency with respect to the gas phase. The model shows that the vibrational lifetime $T_1(\mathrm{OH})$ depends on this redshift $\delta\nu_{\mathrm{OH}}$, according to the relation

$$T_1(\mathrm{OH}) \propto (\delta\nu_{\mathrm{OH}})^{-1.8}. \tag{6}$$

This relation has been verified experimentally for a wide range of hydrogen-bonded complexes[14] and can be understood in the following way. The redshift of the absorption band of the O–H stretch vibration induced by the hydrogen bond is a measure for the strength of the interaction between the hydrogen bond and the O–H stretch vibration. If the interaction gets stronger, the rate of energy transfer to the hydrogen bond will be faster, leading to a shorter T_1. When the temperature is increased, the absorption spectrum of the O–H stretch vibration shifts to the blue, which implies that the average hydrogen-bond strength in water decreases. This explains the increase of T_1 with temperature. By combining Eq. (6) with the known temperature dependence of the O–H absorption band redshift[15], we can describe the T_1 data quite well (see Fig. 5).

The relaxation observed for HDO is to some extent analogous to the relaxation of the O–H stretch vibration of ethanol clusters dissolved in carbon tetrachloride (CCl_4).[16–18] For this system it is also observed that the hydrogen bond is the main accepting mode in the relaxation of the O–H stretch vibration. The energy that is transferred from the O–H stretch vibration to the hydrogen bond causes the hydrogen bond to dissociate, and as a result a transient blueshifted absorption of dissociated ethanol cluster fragments is observed. For this system, the hydrogen-bond reassociation is relatively slow and has a time constant of approximately 20 ps. For water, the relaxation of the hydrogen

bond is much faster and has a time constant $1/k_B$ of approximately 1 ps. A likely reason for the fast hydrogen-bond relaxation in water is that, due to the network of hydrogen bonds, the energy can be dispersed very quickly over the environment of the initially excited molecule. In contrast, in the experiment on ethanol dissolved in CCl_4, the CCl_4 environment does not provide efficient accepting modes, and thus the hydrogen bond relaxes much more slowly.

V. CONCLUSIONS

Using femtosecond mid-infrared pump-probe experiments, we have measured the lifetime of the O–H stretch vibration in liquid HDO in D_2O. For ice-*Ih*, the lifetime has a constant value of 0.37 ± 0.02 ps over the range 33–270 K, while for liquid water, the lifetime increases from 0.74 ± 0.02 ps at 270 K to 0.90 ± 0.02 ps at 363 K. This temperature dependence is quite anomalous since, in general, it is observed that the vibrational lifetime decreases with temperature. If the $0 \rightarrow 1$ transition is probed, it is observed that the relaxation of the bleaching is faster at the blue side of the absorption band than at the center of the absorption band. Both this observation and the anomalous temperature dependence of the vibrational lifetime can be well explained if the O–H$\cdots$O hydrogen bond forms the main accepting mode in the vibrational relaxation of the O–H stretch vibration. From a detailed analysis of the data, we find that the exited hydrogen bond relaxes with a time constant of 1.0 ± 0.5 ps. This relaxation is relatively fast compared to other hydrogen-bonded systems, which can be explained from the fact that the network of hydrogen bonds in liquid water allows a very rapid dissipation of energy.

ACKNOWLEDGMENTS

The work described in this paper is part of a collaborative research program of NIOK (Netherlands Graduate School of Catalysis Research) and FOM (Foundation for Fundamental Research on Matter), which is financially supported by NWO (Netherlands Organization for the Advancement of Research).

[1] H. Graener, G. Seifert, and A. Laubereau, Phys. Rev. Lett. **66**, 2092 (1991).
[2] K. L. Vodopyanov, J. Chem. Phys. **94**, 5389 (1991).
[3] R. Laenen, C. Rauscher, and A. Laubereau, Phys. Rev. Lett. **80**, 2622 (1998).
[4] A. Novak, Struct. Bonding (Berlin) **18**, 177 (1974).
[5] A. Staib and J. T. Hynes, Chem. Phys. Lett. **204**, 197 (1993).
[6] S. Woutersen, U. Emmerichs, H. K. Nienhuys, and H. J. Bakker, Phys. Rev. Lett. **81**, 1106 (1998).
[7] G. M. Gale, G. Gallot, F. Hache, N. Lascoux, S. Bratos, and J.-C. Leickman, Phys. Rev. Lett. **82**, 1068 (1999).
[8] A. Nitzan and J. Jortner, Mol. Phys. **25**, 713 (1973).
[9] R. Laenen, C. Rauscher, and A. Laubereau, J. Phys. Chem. B **102**, 9304 (1998).
[10] U. Emmerichs, S. Woutersen, and H. J. Bakker, J. Opt. Soc. Am. B **14**, 1478 (1997).
[11] H. Graener, G. Seifert, and A. Laubereau, Chem. Phys. Lett. **172**, 435 (1990).
[12] H. Graener, Chem. Phys. Lett. **165**, 110 (1990).
[13] H. Graener and G. Seifert, Chem. Phys. Lett. **98**, 35 (1992).
[14] R. E. Miller, Science **240**, 447 (1988).
[15] T. A. Ford and M. Falk, Can. J. Chem. **46**, 3579 (1968).
[16] H. Graener, T. Q. Ye, and A. Laubereau, J. Chem. Phys. **90**, 1478 (1989).
[17] R. Laenen and C. Rauscher, J. Chem. Phys. **106**, 8974 (1997).
[18] S. Woutersen, U. Emmerichs, and H. J. Bakker, J. Chem. Phys. **107**, 1483 (1997).